DALTON
FULL PAPER

Synthesis, crystal structure and magnetic properties of a novel mixed-valence copper phosphonate: $Na_2Cu_{15}(hedp)_6(OH)_2(H_2O)$ (hedp = 1-hydroxyethylidenediphosphonate)‡

Li-Min Zheng,*,† Chun-Ying Duan, Xiang-Rong Ye, Li-Yi Zhang, Cheng Wang and Xin-Quan Xin

Coordination Chemistry Institute, State Key Laboratory of Coordination Chemistry, Nanjing University, Nanjing 210093, P.R. China

A new pillared layered mixed-valence copper phosphonate $Na_2Cu_{15}(hedp)_6(OH)_2(H_2O)$, where hedp represents 1-hydroxyethylidenediphosphonate anion, has been hydrothermally synthesized and structurally determined. Crystal data: trigonal, space group $P\bar{3}$, $a = b = 11.720(2)$, $c = 9.531(1)$ Å, $U = 1134(2)$ Å^3, $Z = 1$. The structure consists of honeycomb layers of edge-sharing $(Cu^{II}_3O)O_3$ units (sheet A) and edge-sharing NaO_6 octahedra and $Cu^{II}O_4$ planes (sheet B). The layers are pillared alternately through 18-membered rings which are made up from the organic backbone of the diphosphonate groups and the $Cu^{I}O_2$ units. A three-dimensional framework is thus formed which contains intersecting channels where the H_2O molecules reside. The magnetic properties of the compound have been investigated. No long-range ordering has been found down to 2 K.

Recently, metal phosphonate chemistry has received increased attention due to its potential applications in sorption and ion exchange, catalysis and non-linear optics, *etc.*[1] Researches on the copper phosphonates, however, are still limited and most concern monophosphonate compounds.[2–5] Generally, the monophosphonic acids react with metal ions to produce layered compounds in which the metal–O_3PC networks are separated by the organic groups on either side. The interlayer space, therefore, could be adjusted by using different organic groups. The exception for the copper analogues is β-$Cu(CH_3PO_3)$[4] which shows a three-dimensional structure with a channel-type arrangement. By functionally modifying the organic groups, it is possible to build up pillared layered structures, or to provide porous structures.[6–8]

There have been very few studies on the copper diphosphonates up till now. As far as we know, the only two examples are $[Cu_2(O_3PC_6H_4PO_3)(H_2O)_2]$ and $Cu[HO_3P(C_6H_4)_2PO_3H]$.[5] Their structures, which were solved by using X-ray powder diffraction data, revealed lamellar layered arrangements where the adjacent layers of Cu–O_3P (or Cu–HO_3P in the latter case) are covalently pillared by the phenyl or biphenyl groups. Employing hydrothermal techniques, we have synthesized a novel mixed-valence copper(I/II) diphosphonate compound $Na_2Cu_{15}(hedp)_6(OH)_2(H_2O)$ (hedp = 1-hydroxyethylidenediphosphonate). It is, to the best of our knowledge, the first example of a mixed-valence copper phosphonate. A single-crystal structure determination demonstrated a new pillared layer structure, with two different kinds of sheets arranged alternately. A detailed structural description as well as the magnetic behaviour of the compound is presented.

Experimental

Materials and methods

All starting materials were reagent grade used as purchased. The elemental analysis was performed on a PE 240C elemental analyzer. The infrared spectrum was recorded on a Fourier Nicolet FT-170 SX spectrophotometer with pressed KBr pellets. X-Ray photoelectron spectroscopy (XPS) was performed with an ESCALAB MK-II electron spectrometer.

† E-Mail: lmzheng@netra.nju.edu.cn

‡ *Non-SI units employed*: eV ≈ 1.60×10^{-19} J, G = 10^{-4} T, $\mu_B \approx 9.27 \times 10^{-24}$ J T^{-1}.

Synthesis of $Na_2Cu_{15}(hedp)_6(OH)_2(H_2O)$ 1

The compound was first prepared by hydrothermal treatment of $Cu(NO_3)_2 \cdot 3H_2O$ (1 mmol), 50% hedp (1 cm^3) and 1 M NaOH (8 cm^3) for 60 h at 180 °C. Brown crystals of **1**, suitable for single crystal structural determination, were obtained as a minor phase together with unidentified blue plate-like crystals. Replacement by a mixture of $Cu(NO_3)_2 \cdot 3H_2O$ (1 mmol), 50% hedp (1 cm^3), 1 M NaOH (7 cm^3) and 1,4-diazabicyclo[2.2.2]-octane (dabco) (1 mmol) yielded a single phase of **1**, as judged by comparison of the powder X-ray diffraction of the bulk product with the pattern simulated from coordinates derived from the single-crystal study. The XPS spectrum of the powder sample suggested the existence of Cu^{I} in the compound according to the $^2p_{\frac{3}{2}}$ peak at 933.2 eV. The evident shoulder peaks at 935.8 and 938.2 eV, as well as the characteristic shake-up satellite peaks in the high binding energy extremities of the $^2p_{\frac{3}{2}}$ and $^2p_{\frac{1}{2}}$ peaks confirmed that the compound also contains copper(II) ions in two different environments. This result was confirmed by the single-crystal structural determination. No nitrogen atoms were detected by XPS (Found: C, 6.91; H, 1.67. Calc.: C, 6.36; H, 1.24%). IR (KBr): 3487m, 3483m, 3159s (br), 1433s, 1367s, 1091vs, 999vs, 935s, 818s, 683s, 608s, 569s, 502s and 429s cm^{-1}.

Crystallography

A crystal with dimensions 0.50 × 0.40 × 0.20 mm was selected for indexing and intensity data collection at 293(2) K on a Siemens P4 four-circle diffractometer with monochromated Mo-Kα (λ = 0.710 73 Å) radiation. Cell constants and an orientation matrix for data collection were obtained from least-squares refinement of the setting angles of 11 randomly oriented reflections in the range $4.74 \leqslant \theta \leqslant 8.83$, corresponding to a monoclinic cell. As a check on crystal and instrument stability, three representative reflections were measured every 100, and a decay of 5.18% was observed. Intensity data were collected using the θ–2θ scan mode with a variable scan speed 5.0–50.0° min^{-1} in ω. The data were corrected for Lorentz-polarization effects during data reduction using XSCANS.[9] An empirical absorption correction based on ψ-scan measurements was applied, which resulted in transmission factors ranging from 0.34 to 0.88.

The structure was solved by direct methods and refined on F^2 by full-matrix least squares using SHELXTL.[10] All the non-

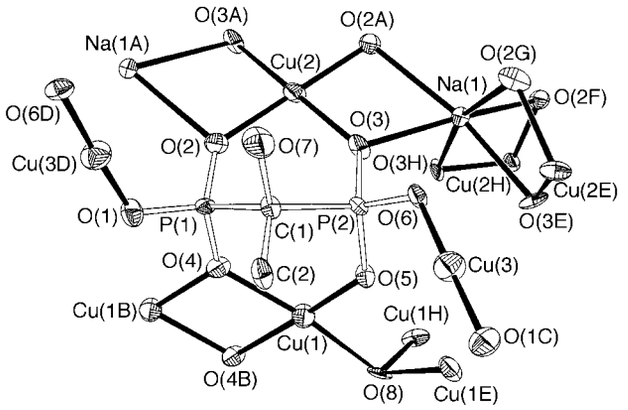

Fig. 1 Co-ordination geometries of copper and sodium in compound **1**, showing the atomic labeling scheme. Thermal ellipsoids are at the 50% probability level

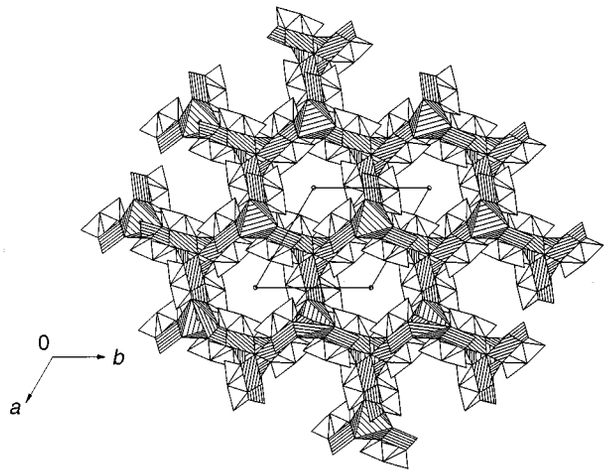

Fig. 2 Polyhedral representation of the structure of compound **1** packed along the [001] direction. All the H, C(2), O(7) and Cu(3) atoms are omitted for clarity

hydrogen atoms were refined anisotropically. The hydrogen atoms of the methyl and hydroxy groups were placed in calculated positions (C–H 0.96 Å) and allowed to ride on their respective parent atoms. The H atom in H_2O was found from the Fourier-difference map. All the hydrogen atoms were assigned fixed isotropic thermal parameters 1.5 times the equivalent isotropic U of the atoms to which they are attached. The contributions of these hydrogen atoms were included in the structure-factor calculations. In the final Fourier-difference map the deepest hole was -1.287 e Å^{-3}, the highest peak 1.906 e Å^{-3} located near Cu(1) (1.075 Å).

All computations were carried out on a PC-586 computer using the SHELXTL package. Analytical expressions of neutral-atom scattering factors and anomalous dispersion corrections were incorporated.[11] Crystallographic data are summarized in Table 1, selected bond lengths and angles in Table 2.

CCDC reference number 186/842.

See http://www.rsc.org/suppdata/dt/1998/905/ for crystallographic files in .cif format.

Magnetic measurements

Variable-temperature magnetic susceptibility data were obtained on a polycrystalline sample (22.6 mg) from 2 to 300 K in a magnetic field of 5 kG after zero-field cooling using a SQUID magnetometer. Diamagnetic corrections were estimated from Pascal's constants.

Results and Discussion

Crystal structure

Fig. 1 illustrates the co-ordination of the Cu and Na, together with the labelling scheme. Clearly, three kinds of copper atoms are crystallographically distinguished, among which Cu(2) sits on an inversion center. The diphosphonate group acts as a multidentate bridging ligand to chelate the Cu(1) and Cu(2) atoms using its four terminal PO_3 oxygen atoms. The remaining two oxygen atoms of PO_3 co-ordinate to Cu(3). Both Cu(1) and Cu(2) are bivalent and four-co-ordinated. The Cu(1)O_4 arrangement is distinctly more distorted, with the shortest Cu(1)–O(5) bond length 1.927(7) Å and the longest Cu(1)–O(4B) 2.040(8) Å. Atom Cu(1) is pulled out of the plane, defined by O(4), O(4B), O(5) and O(8), by 0.128(2) Å. The Cu(2) atom is centrosymmetrically co-ordinated to four oxygen atoms with a mean Cu–O of 1.960(8) Å. The Cu(3) atom is monovalent and two-co-ordinated. The Cu(3)O_2 unit is distorted from a linear geometry with a bond angle of 177.8(4)°. The Cu(3)–O bond distances [1.822(9), 1.825(8) Å] are slightly longer than 1.81 Å, the sum of the Shannon crystal radii of 0.60 Å for two-co-ordinated Cu^+ and 1.21 Å for two-co-ordinated O^{2-}.[12]

The Na, which is edge-shared with Cu(2), has a distorted octahedral environment (Fig. 1). The Na–O distances, mean 2.442(8) Å, can be compared with those in $NaCu(O_2CCH_2NHCH_2PO_3)(H_2O)_{3.5}$.[6]

The structure of $Na_2Cu_{15}(hedp)_6(OH)_2(H_2O)$ consists of alternately arranged layers of $[Cu(1)_3O(8)]O_3$ (sheet A) and $Cu(2)O_4Na(1)$ (sheet B) along the [001] direction. Both Na(1) and O(8) are at special positions of three-fold axes. The spaces between the layers are filled with the organic backbone of the hedp groups as well as $Cu(3)O_2$ units, forming intersecting channels parallel to the ⟨001⟩ directions in which the H_2O molecules reside (Fig. 2).

Fig. 3(*a*) emphasizes the honeycomb layer A created by the Cu(1) atoms, OH groups and the co-ordinated phosphonate atoms. Three equivalent Cu(1) atoms can be found with the μ_3–O(8) atom centered above an equilateral triangle. The deviation of O(8) atom from this triangle plane is 0.728(1) Å. Each triangular Cu(1) cluster is centrosymmetrically attached to the other through edge-sharing co-ordination in three directions. Subsequently, a distinct two-dimensional $(Cu_3O)O_3$ network is constructed with 12-membered rings. Similar 12-ring cavities are found in the honeycomb layer B which is generated from the edge-shared $Cu(2)O_4$ planes and $Na(1)O_6$ octahedra [Fig. 3(*b*)]. The interlayer distance is equal to half of the *c*-axis parameter (4.766 Å).

It is interesting that the organic backbone of hedp groups combines with the Cu(3) atoms to form nine-membered rings (Fig. 4). These rings are sandwiched between Sheets A and B, and are placed in such a way that intersecting channels are produced along the [001] direction (Fig. 2). The lattice water molecules, sitting on three-fold axes, are centered inside the channels and stabilized through hydrogen-bonding to the unco-ordinated OH groups from three diphosphonate groups. The distance of O(1W)···O(7) is 2.561(6) Å.

Magnetic properties

The temperature dependence of the magnetic susceptibility was measured in the temperature range 300 to 2 K. The magnetic behaviour is shown in Fig. 5 in the forms of plots of χ_m *vs.* T and $\chi_m T$ *vs.* T, respectively. At 300 K the magnetic moment (μ_{eff}) per copper(II) atom, determined from the equation $\mu_{eff} = 2.828(\chi_m T)^{\frac{1}{2}}$, is 1.56 μ_B which is lower than expected for an isolated paramagnetic system with $S = \frac{1}{2}$ ($\mu_{eff} = 1.73\mu_B$). Upon cooling, $\chi_m T$ decreases and tends to stabilize below 80 K and then below 40 K it decreases abruptly reaching a value of 0.66 cm^3 K mol^{-1} at 2 K, indicating an antiferromagnetic interaction.

As described, the structure of the compound is composed of

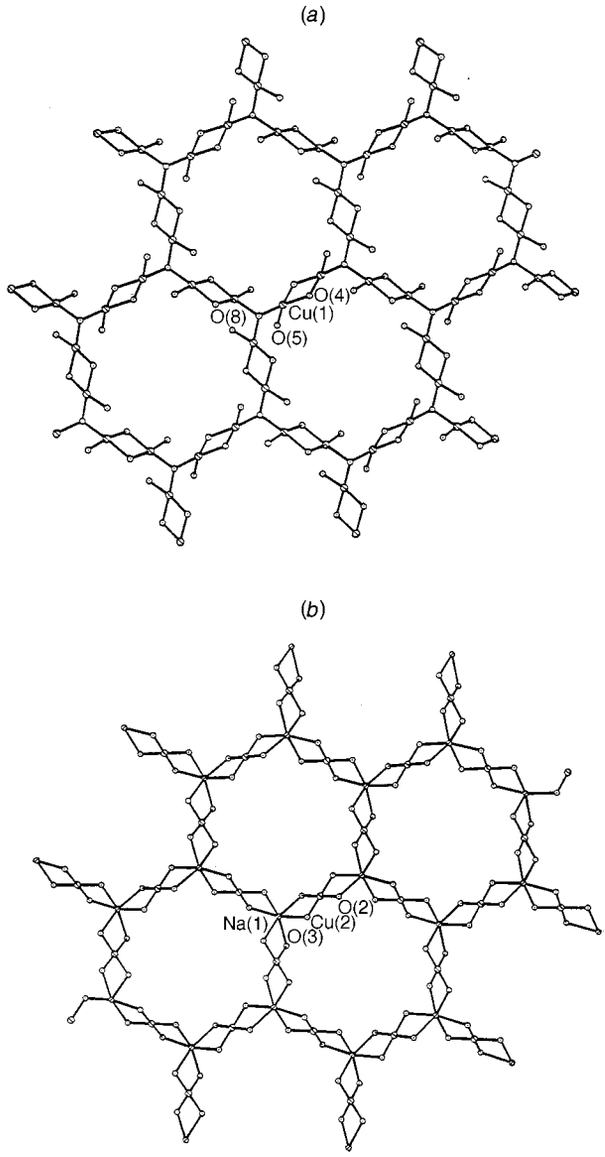

Fig. 3 Sheets A (*a*) and B (*b*) of structure **1** viewed along the *c* axis

sheets A and B which are arranged alternately along the [001] direction. Between the neighboring sheets are diamagnetic organic groups and monovalent Cu(3). In sheet B, the magnetically active Cu(2) is isolated by the electron-localized O–Na–O bridges [Cu(2)···Cu(2A) 5.860(6) Å] (Fig. 1) and exchanges between Cu(2) centers can be neglected. The antiferromagnetic interactions, therefore, should be mainly attributed to sheet A. As for the coupling between Cu(1) ions in sheet A, two exchange pathways are possible: one through the centered μ_3-O(8)H and the other through phosphonate bridges involving O(4) and O(4B) (Fig. 1).

On the one hand hydroxo-bridges are known to be efficient in transmitting antiferromagnetic exchange interaction between two copper(II) ions. Hatfield and co-workers[13] investigated the magnetostructural correlation of some dihydroxo-bridged copper(II) dimers and found that with varying bridging angle Cu–O–Cu (α) from 95.6 to 104.1°, the singlet–triplet energy gap J varied in parallel from +172 to −509 cm^{-1}. They deduced a linear correlation between J and α, which predicts that a larger α value would lead to a more pronounced antiferromagnetic interaction. In the present case, the Cu···Cu distances through the μ_3-O(8)H and O(4) bridges are 3.256 and 3.219 Å, respectively, which excludes possible direct exchanges between the copper(II) atoms. Further, the Cu(1)–O(8)–Cu(1E) bridging angle [107.7(4)°] is larger than Cu(1)–O(4)–Cu(1B) [104.5(4)°], which could result in a predominant antiferromagnetic coupling within the $Cu(1)_3O(8)$ triangle. On the other hand, the exchange coupling between magnetic ions in a regular triangle arrangement is known to be subject to strong spin frustration interfering with the magnetic ordering.[14] The lack of a maxi-

Table 1 Crystallographic data for $Na_2Cu_{15}(hedp)_6(OH)_2(H_2O)$

Formula	$C_{12}H_{28}Cu_{15}Na_2O_{45}P_{12}$
M	2263.28
Crystal system	Trigonal
Space group	$P\bar{3}$
a/Å	11.720(2)
c/Å	9.531(1)
U/Å^3	1134(2)
Z	1
D_c/g cm^{-3}	3.315
$F(000)$	1097
μ(Mo-Kα)/cm^{-1}	74.51
Maximum 2θ/°	50
Reflections collected	1938
Independent reflections	1320 (R_{int} = 0.0476)
T_{min}, T_{max}	0.3416, 0.8801
Data, restraints, parameters	1308, 0, 132
Goodness of fit on F^2	1.069
$R1$, $wR2$ [$I > 2\sigma(I)$]	0.0565, 0.1384
(all data)	0.0939, 0.1659
$(\Delta\rho)_{max}$, $(\Delta\rho)_{min}$/e Å^{-3}	1.906, −1.287

$R1 = \Sigma||F_o| - |F_c||/\Sigma|F_o|$, $wR2 = [\Sigma w(F_o^2 - F_c^2)^2/\Sigma w(F_o^2)^2]^{\frac{1}{2}}$.

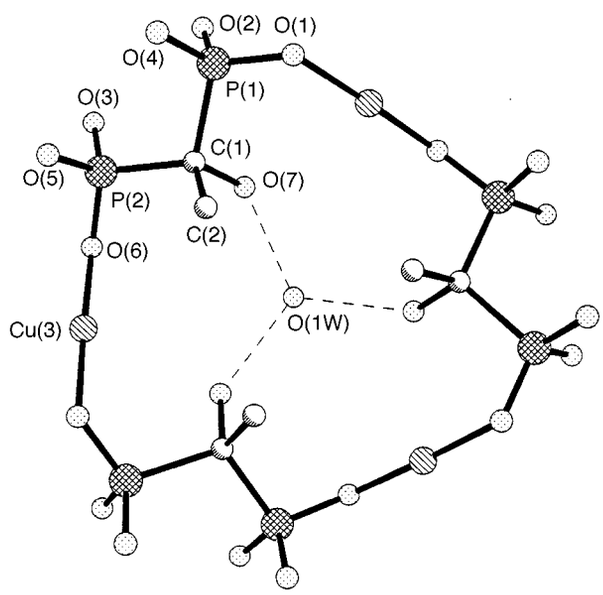

Fig. 4 A nine-membered ring containing a H_2O molecule viewed along the *c* axis. Hydrogen-bonding interactions are shown as dashed lines

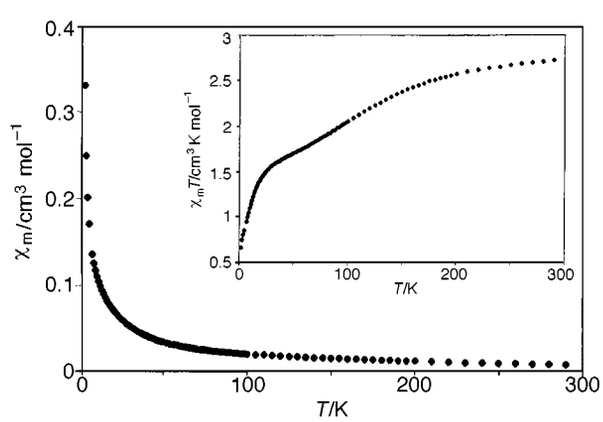

Fig. 5 Molar magnetic susceptibility (χ_m, $\chi_m T$) *versus* temperature curves for compound **1**

Table 2 Selected bond lengths (Å) and angles (°) for $Na_2Cu_{15}(hedp)_6(OH)_2(H_2O)$

Cu(1)–O(4)	2.032(7)	Cu(1)–O(5)	1.927(7)
Cu(1)–O(4B)	2.040(8)	Cu(1)–O(8)	2.016(5)
Cu(2)–O(2)	1.967(8)×2	Cu(2)–O(3)	1.952(8) ×2
Cu(3)–O(1C)	1.822(9)	Cu(3)–O(6)	1.825(8)
Na(1)–O(3)	2.402(8)×3	Na(1)–O(2A)	2.481(8) ×3
P(1)–O(1)	1.521(8)	P(1)–O(2)	1.501(9)
P(1)–O(4)	1.516(8)	P(2)–O(3)	1.522(8)
P(2)–O(5)	1.525(8)	P(2)–O(6)	1.525(8)
P(1)–C(1)	1.842(11)	P(2)–C(1)	1.827(10)
C(1)–O(7)	1.458(13)	C(1)–C(2)	1.480(20)
O(4)–Cu(1)–O(4B)	75.5(4)	O(4)–Cu(1)–O(5)	97.5(3)
O(4)–Cu(1)–O(8)	171.7(4)	O(4B)–Cu(1)–O(5)	170.6(3)
O(4B)–Cu(1)–O(8)	101.5(4)	O(5)–Cu(1)–O(8)	84.6(4)
O(2)–Cu(2)–O(2A)	180.0(1)×2	O(2)–Cu(2)–O(3)	93.2(3)×2
O(2)–Cu(2)–O(3A)	86.8(3)×2	O(6)–Cu(3)–O(1C)	177.8(4)
O(3)–Na(1)–O(2A)	66.9(3)×3	O(3)–Na(1)–O(3E)	97.3(3)×3
O(3)–Na(1)–O(2F)	163.6(3)×3	O(2A)–Na(1)–O(2F)	107.1(3)×3
O(3)–Na(1)–O(2G)	89.3(2)×3	Cu(1)–O(8)–Cu(1E)	107.7(4)×3
Cu(1)–O(4)–Cu(1B)	104.5(4)	Cu(2)–O(2)–Na(1A)	100.1(4)
Cu(2)–O(3)–Na(1)	103.2(3)	Cu(1)–O(4)–P(1)	131.5(5)
Cu(1)–O(5)–P(2)	128.5(4)	Cu(1B)–O(4)–P(1)	123.9(4)
Cu(2)–O(2)–P(1)	135.0(5)	Cu(2)–O(3)–P(2)	137.1(5)
Cu(3D)–O(1)–P(1)	121.3(5)	Cu(3)–O(6)–P(2)	125.7(5)
Na(1)–O(3)–P(2)	119.3(4)	Na(1A)–O(2)–P(1)	124.0(5)
O(1)–P(1)–O(2)	113.6(5)	O(1)–P(1)–O(4)	107.8(5)
O(1)–P(1)–C(1)	109.3(4)	O(2)–P(1)–O(4)	111.8(5)
O(2)–P(1)–C(1)	107.2(5)	O(4)–P(1)–C(1)	106.9(5)
O(3)–P(2)–O(5)	115.3(4)	O(3)–P(2)–O(6)	109.7(5)
O(3)–P(2)–C(1)	108.2(5)	O(5)–P(2)–O(6)	110.2(4)
O(5)–P(2)–C(1)	104.8(5)	O(6)–P(2)–C(1)	108.3(4)
P(1)–C(1)–C(2)	110.2(8)	P(1)–C(1)–O(7)	107.9(7)
P(1)–C(1)–P(2)	109.6(5)	P(2)–C(1)–C(2)	110.0(8)
P(2)–C(1)–O(7)	111.2(8)	C(2)–C(1)–O(7)	107.9(8)

Symmetry codes: A $1-x, 1-y, 1-z$; B $1-x, 1-y, 2-z$; C $2-y, 1+x-y, z$; D $1-x+y, 2-x, z$; E $1-x+y, 1-x, z$; F $y, y-x, 1-z$; G $1+x-y, x, 1-z$

mum in the χ_m *vs.* T plot suggests that no long-range ordering is achieved down to 2 K. Additionally, the equilateral triangular arrangement should result in a ground state with one unpaired electron when the temperature is low. Taking into account such a ground state in sheet A and the isolated Cu(2) in sheet B, the expected μ_{eff} per molecule is 3.87 μ_B, in agreement with the experimental value of 3.68 μ_B at 50 K. The further decrease of $\chi_m T$ below 40 K could be due to the superexchange interactions between Cu(2) ions within sheet B, and/or between Cu(1) and Cu(2) ions through diamagnetic interlayer spaces.

Acknowledgements

The authors are deeply indebted to Dr. Kwang-Hwa Lii, Institute of Chemistry, Academia Sinica, Taipei, for the magnetic susceptibility and powder X-ray diffraction measurements and valuable comments.

References

1 A. Clearfield, *New Developments in Ion Exchange Materials*, eds. M. Abe, T. Kataoka and T. Suzuki, Kodansha, Ltd., Tokyo, 1991. B. Z. Wan, R. G. Anthony, G. Z. Peng and A. Clearfield, *J. Catal.*, 1994, **101**, 19; G. Cao, H. Hong and T. E. Mallouk, *Acc. Chem. Res.*, 1992, **25**, 420.
2 Y. Zhang and A. Clearfield, *Inorg. Chem.*, 1992, **31**, 2821.
3 J. Le Bideau, B. Bujoli, A. Jouanneaux, C. Payen, P. Palvadeau and J. Rouxel, *Inorg. Chem.*, 1993, **32**, 4617.
4 J. Le Bideau, C. Payen, P. Palvadeau and B. Bujoli, *Inorg. Chem.*, 1994, **33**, 4885.
5 D. M. Poojary, B. Zhang, P. Bellinghausen and A. Clearfield, *Inorg. Chem.*, 1996, **35**, 4942.
6 E. T. Clark, P. R. Rudolf, A. E. Martell and A. Clearfield, *Inorg. Chim. Acta*, 1989, **164**, 59.
7 S. Drumel, P. Janvier, P. Barboux, M. Bujoli-Doeuff and B. Bujoli, *Inorg. Chem.*, 1995, **34**, 148.
8 S. Drumel, P. Janvier, M. Bujoli-Doeuff and B. Bujoli, *Inorg. Chem.*, 1996, **35**, 5786.
9 XSCANS, (version 2.1), Siemens Analytical X-ray Instruments, Madison, WI, 1994.
10 *SHELXTL* (*version* 5.0) *Reference Manual*, Siemens Industrial Automation, Analytical Instrumentation, Madison, WI, 1995.
11 *International Tables for X-Ray Crystallography*, ed. A. J. C. Wilson, Kulwer, Dordrecht, 1992, vol. C.
12 R. D. Shannon, *Acta Crystallogr.*, *Sect. A*, 1976, **32**, 751.
13 W. H. Crawford, H. W. Richardson, J. R. Wasson, D. J. Hodgson and W. E. Hatfield, *Inorg. Chem.*, 1976, **15**, 2107.
14 R. S. Gekht, *Sov. Phys. JETP*, 1992, **75**, 1058. G.-G. Linder, M. Atanasov and J. Pebler, *J. Solid State Chem.*, 1995, **116**, 1.

Received 10*th September* 1997; *Paper* 7/06601E